

Edge-guided Non-local Fully Convolutional Network for Salient Object Detection

Zhengzheng Tu, Yan Ma, Chenglong Li, Jin Tang, Bin Luo

Abstract—Fully Convolutional Neural Network (FCN) has been widely applied to salient object detection recently by virtue of high-level semantic feature extraction, but existing FCN-based methods still suffer from continuous striding and pooling operations leading to loss of spatial structure and blurred edges. To maintain the clear edge structure of salient objects, we propose a novel Edge-guided Non-local FCN (ENFNet) to perform edge-guided feature learning for accurate salient object detection. In a specific, we extract hierarchical global and local information in FCN to incorporate non-local features for effective feature representations. To preserve good boundaries of salient objects, we propose a guidance block to embed edge prior knowledge into hierarchical feature maps. The guidance block not only performs feature-wise manipulation but also spatial-wise transformation for effective edge embeddings. Our model is trained on the MSRA-B dataset and tested on five popular benchmark datasets. Comparing with the state-of-the-art methods, the proposed method achieves the best performance on all datasets.

Index Terms—Salient object detection, edge guidance, non-local features, fully convolutional neural network

I. INTRODUCTION

SALIENCY detection is generally divided into two categories: salient object detection or eye fixation prediction, with the purpose of extracting the most predominant objects or predicting human eye attended locations corresponding to informative regions in an image. With the rapid development of deep learning, saliency detection has made great progress in recent years. As a preprocessing step, saliency detection is helpful for many applications in the computer vision tasks, such as image segmentation [1], [2], [3], scene classification [4], visual tracking [5], [6], [7], and person re-identification [8].

The saliency of each region is usually defined as the weight of the distance between the region and other regions of the image in most traditional methods, and often based on hand-crafted features and some priors [9], [10], [11]. In recent years, with the success of Fully Convolutional Network (FCN) in the field of computer vision, deep learning methods has become a promising alternative to salient object detection.

Z. Tu, Y. Ma, C. Li, J. Tang, and B. Luo are with Key Lab of Intelligent Computing and Signal Processing of Ministry of Education, School of Computer Science and Technology, Anhui University, Hefei 230601, China, Email: zhengzhengahu@163.com, m17856174397@163.com, lc1314@foxmail.com, tangjin@ahu.edu.cn. C. Li is also with Institute of Physical Science and Information Technology, Anhui University, Hefei 230601, China. (Corresponding author is Chenglong Li)

This research is jointly supported by the National Natural Science Foundation of China (No. 61602006, 61702002, 61872005, 61860206004), Natural Science Foundation of Anhui Province (180805QF187), Open fund for Discipline Construction, Institute of Physical Science and Information Technology, Anhui University.

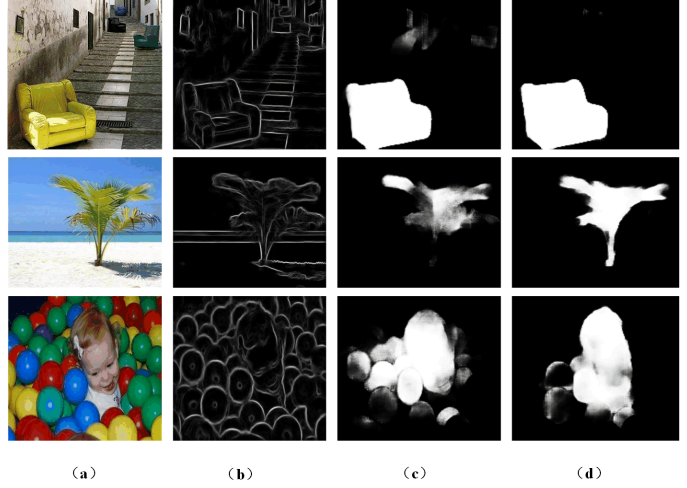


Fig. 1. Illustration of the importance of edge information to saliency detection performance. (a) Input images. (b) Edge maps. (c) Saliency results without edge embeddings. (d) Saliency results with edge embeddings.

Existing methods based on the FCN [12], [13], [14], [15], [16], [17], [18], [19], [20] have shown good performance, since the features obtained at deeper layers typically contain stronger semantic information and the global context-aware information, which are beneficial to locate salient regions even in complex scenes. FCN promotes saliency detection by applying multiple convolution layers and pooling layers to increase the receptive field and automatically extract high-level semantic information, which plays an import role in this field. These continuous convolution layers and pooling operations gain large receptive fields and high representation ability but reduce the size of feature maps and lose the spatial structure, and deteriorate the edges of the salient objects. This is useful for high-level tasks, but unfortunately, it reduces the accuracy of low-level tasks which usually requires precise pixel activation, such as salient object boundaries.

Some recent works notice this problem and propose some edge-aware saliency detection methods. For example, Zhang *et al.* [18] embed edge-aware feature maps achieved by shadow layers into the deep learning framework. Mukherjee *et al.* [21] construct a Bayesian probabilistic edge mapping which uses low-order edge features to assign a saliency value to the edge. However, boundary preserving still hasn't been solved well as lack of specific guide for the boundary area.

In [22], the image is segmented into several regions by hand-craft features. The hand-craft low-level features and the CNN high-level feature can complement each other. [12] extracts

the hand-craft features to compute the salient value of each super-pixel. However, these hand-crafted low-level features are incapable to capture high-level semantic features of the salient objects.

Though good performance are achieved, it still suffers from a major problems shown in Fig. 1(c):the predictions around object boundaries are inaccurate due to the essential fine details(low-level visual cues) loss caused by repeated strides and pooling operations. In a word, existing FCN-based methods still have the drawback that they are difficult to maintain spatial structure, for example, clear edge structure.

In order to solve the problem of the ambiguous boundary of salient objects, and inspired by [23], which employs the possibility of semantic segmentation maps as the categorical prior to guide the recovery of realistic texture in image super-resolution, we take the FCN model(NLDF) [20] as our baseline. To maintain the clear edge structure of salient objects and preserve good boundaries of salient objects, we propose a novel Edge-guided Non-local FCN (ENFNet) to perform edge-guided feature learning for accurate salient object detection. What's more, we propose a edge guidance block to combine hierarchical feature and edge prior knowledge to capture distinctive objectness and detailed information simultaneously. The guidance block not only performs feature-wise manipulation but also spatial-wise transformation for effective edge embeddings. In a specific, we feed two images into our network, the two input images are collected from salient object detection and edge image generated by the edge detection method [24]. Through adding the edge prior to NLDF [20] and fusing edge feature and hierarchical features in an embedded way, the network takes advantage of good edge detection to help achieve better salient object detection result. Extensive experiments have proved that embedding the edge prior information to the network is effective, the network can produce good saliency maps with clear boundaries. An example of edge information and generated saliency maps by our method are shown in Fig. 1.

In short, the major contributions of this work are summarized as follow:

- We propose a novel Edge-guided Non-local FCN (ENFNet), which edge guidance block can provide more detailed edge information in the process of saliency detection, to perform edge-guided feature learning for accurate salient object detection. The proposed approach has better performance than the baseline approach.
- We compare the proposed approach with many start-of-the-art saliency detection methods on the five benchmark datasets: HKU-IS [25], PASCAL-S [26], DUT-OMRON [10], ECSSD [11] and SOD [27]. Our method achieves the best performance under different evaluation metrics.

II. RELATED WORK

We will review two aspects of salient object detection approaches, that are deep learning based salient object detection and exploiting edge information salient object detection.

Deep learning based methods. Salient object detection can be regarded as a pixel-wise classification problem. Although traditional salient object detection methods have their superiority, including no need training and simplicity, their overall performances are not as good as most deep learning methods. Deep learning based methods have achieved great improvement in salient object detection,as they combine local and deep features and can be trained end-to-end.

In the state-of-the-art models of convolutional neural net(CNN), feature selection between salient and non-salient regions is automatically accomplished by gradient descent. These models are made of a series of convolution layers and pooling until a softmax layer, which predicts the probability of each pixel belonging to objects. Recently, these methods make a great process by deep learning methods [25], [28], [29], [12], [13], [14], [15], [16], [17], [18], [19], which can be divided into region-based and Fully Convolutional Networks(FCN)-based methods.

The region-based deep learning method uses image patches as the basic processing units for saliency prediction. For example, Li et al. [25] utilize multi-scale features to capture contextual information and a classifier network to infer the saliency of each image segment.Zhao et al. [30] propose a multi-context deep CNN framework benefiting from the global context of salient objects, as global context is conducive to modeling saliency of the image, while local context is conducive to estimating saliency of the region with rich features. Li et al.[15] propose a deep contract network to combine a piece-wise stream and a pixel-level stream for saliency detection. And Wang et al. [31]propose to train two deep neural networks to integrate global search and local estimation for salient object detection. The work in [12] use a two stream framework to separately extract high-level features from VGG-net and low-level features such as color histogram. The fully-connected layers in CNNs is always to evaluate the saliency of every region [32]. The region-based methods improve the performance over the ones based on hand-crafted features to a great extent, whereas they ignore the important spatial information. In addition, the region-based methods are time-consuming, as the network has to run many times.

In order to improve the problem of time-consuming of CNN methods, people utilize FCN to generate a pixel-wise prediction. The FCN methods abandoned the fully connected layer in CNN, though they can increase the computational efficiency, whereas lost the spatial information. For example, Li et al. [15] make use of segment-level spatial pooling stream and pixel-level fully convolutional stream to generate saliency estimation. The work in [28] design a deep recurrent FCN to incorporate the coarse estimations as saliency priors and refine the generated saliency stage by stage. In HED [34], the authors build skip-connections to employ multi-scale deep features for edge detection. The edge detection task is easier than saliency detection since it does not rely on much high-level semantic information. Thus, directly using skip-connections in salient object detection is unsatisfactory. Then, Hou et al. [35] propose dense short connections to skip-layers within the HED architecture to get rich multi-scale features for salient object detection. Another work by SRM [36] proposes a

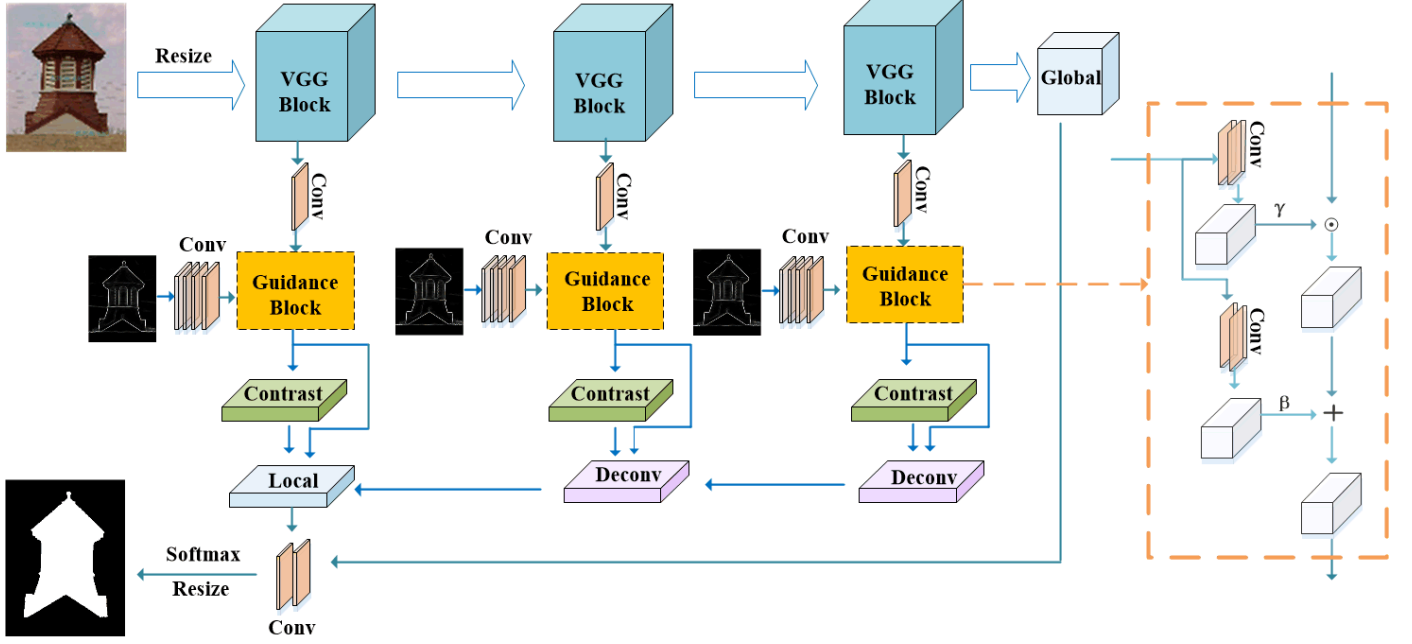


Fig. 2. The overall architecture of our proposed model. Our architecture is based on VGG-16 [33] for better comparison with previous CNN-based methods. Here, only three convolution blocks are listed for illustration. The dotted-line part is a Guidance Block. The edge feature as a condition information into the Guidance block, and transmits the edge information to the next layer of the network in an embedded way.

pyramid pooling model and a stage-wise refinement model to integrate both global and local context information. zhang et al. [18] aggregate high level and low level features by concatenating feature maps directly, these multi-level features are beneficial to recover local details and locate salient objects. In addition, many methods attempt to find a way to fuse multi-scale features for better distinguishing salient and non-salient regions. However, supervised by ground truth and without edge information, they can roughly detect the targets but cannot uniformly highlight the entire objects, and the estimated saliency maps suffer from the blur boundary.

Exploiting Edge Information. To solve above-mentioned blurred boundary problem, some methods attempt to take advantage of edge information for generating saliency maps with clear boundaries. Mukherjee et al. [21] construct a Bayesian probabilistic edge mapping and assign a salient value to the edge by using low-order edge features, then they learn a conditional random field to effectively combine these features with object/non-object labels for edge classification. The work in [37] and [38] use edge information for detecting salient regions. For example, in [37], firstly, they exploit a pre-trained edge detection model to detect the edge of objects. Secondly, based on the detected edge, they segment the image into regions, and generate saliency map of every region through a mask-based Fast R-CNN [39]. The model in [40] uses three different labels: salient objects, salient object's boundaries and background. And in [41] add a edge detection branch into the pooling network, through joint training saliency model and edge detection, the details of salient objects are further sharpened. To emphasize the accuracy of saliency boundary detection, the model [40] takes the extra hand-craft edge feature as a complementary to preserve edge information effectively.

Guan et. al [42] proposes an edge detection stream to combine multiple side outputs together through concatenation and uses a fusion layer that a 1×1 convolution to get the unified output. With the edge information added, these above models get success in preserving the boundary of salient object.

So, we propose a novel Edge-guided Non-local Fully ConvNet (ENFNet) to perform edge-guided feature learning. In a specific, we extract hierarchical global and local information in FCN to incorporate non-local features for effective feature representations. To preserve good boundaries of salient objects, we propose a guidance block to embed edge prior knowledge into hierarchical feature maps. The guidance block not only performs feature-wise manipulation but also spatial-wise transformation for effective edge embeddings. As a result, our method can accurately detect the objects and uniformly highlight the objects, and the estimated saliency map has more clear boundaries.

III. EDGE-GUIDED NON-LOCAL FULLY CONVNET

In this section, we will introduce the network structure of we proposed Edge-guided Non-local Fully ConvNet(ENFNet). The overall structure of the proposed network is shown in Fig. 2.

A. Overview of Network Architecture

As mentioned in section two, a good saliency detection model can combine global context information and local structure information with different resolution details, and different resolution features can better locate the boundary of the salient object. To detect salient objects accurately, existing methods usually use complex backbone network architectures to learn and fuse features. To avoid these problems, the

network NLDF [20] proposed a simple network structure, each column of the network extracts different resolution features. The image size of the input model is 352×352 , and the output saliency map is 176×176 . To obtain a saliency map of the same size as the input image, using a bilinear interpolation method. However, when the foreground and background have the same contrast, and the object has a complex background, the predicted results are often not so good, such as not clear boundaries. Therefore, to preserve good boundaries of salient objects, we propose Edge-guided Non-local Fully ConvNet, which guidance block to embed edge prior knowledge into hierarchical feature maps for effective feature representations. The edge prior knowledge is beneficial to guide the results of saliency detection to possess good object boundaries as shown in Fig. 1.

As shown in Fig. 2, the proposed network is built on the NLDF [20] and choose VGG-16 [33] as our backbone network. Here, we don't use the fully-connected layer because the task of saliency detection is focused on pixel-level prediction. We select VGG-16 first five block as side outputs. Each side output is followed by a convolution block, which is designed to obtain hierarchical multi-scale features $\{X_1, X_2, X_3, X_4, X_5\}$. The revised VGG-16 net provides feature maps at five stages. Every convolution blocks contain two or three convolution layer and a max pooling operation. The last block behind the backbone network contains three convolutional layers to computes global features X_G that is the global context of the image.

The middle layer is we proposed guidance block, which is located on the right side of Fig. 2. Details of guidance block as shown in Table I. Firstly, we extract edge maps using the existing method[24]. The edge maps are used as input of Condition Network and output edge features X_i^E . Secondly, edge feature X_i^E and hierarchical multi-scale features $X_i (i \in \{1, 2, 3, 4, 5\})$ are fused by guidance block. Finally, the edge features X_i^F after fusion are obtained, as shown in Fig 2. Further, through average pooling operation on X_i^F to obtain the contrast features X_i^c . Because the salient object is related to global or local contrast, the contrast feature captures the difference between each feature and its neighbors and it prefers the region lighter or darker than itself.

The last line of our model is a series of deconvolution blocks, these deconvolution operations update the features maps from 11×11 to 176×176 , for the convenience of concatenating feature maps(X_i^F, X_i^c) with different scale. The Local blocks contains one convolution layer to computes the local feature X_L . Finally, in the last line we use two convolution layers and a softmax operation to compute the score of the predicted saliency map by fusing the local and global features.

B. Hierarchical Non-local Structure

Some works show that lower layers in convolutional neural networks can capture rich spatial information, while higher layers encode object-level information but are invariant to factors such as appearance and pose [43]. Generally speaking, the receptive field of lower layers is limited, it is unreasonable

TABLE I
DETAILS OF PROPOSED DEEP CONVOLUTIONAL NETWORKS FOR
GUIDANCE BLOCK.

Block	Layer	kernal	S	Pad	Output
CN	4 conv	3*3	1	Yes	176*176*128
Guidance Block-1	2 conv	3*3	1	Yes	176*176*128
Guidance Block-2	2 conv	3*3	2	Yes	88*88*128
Guidance Block-3	2 conv	3*3	2	Yes	44*44*128
Guidance Block-4	2 conv	3*3,5*5	2,4	Yes	22*22*128
Guidance Block-5	2 conv	5*5	4	Yes	11*11*128

to require the network to perform dense prediction in the early stage. Performing feature extraction instead of feature classification at earlier stages, those extracted low-level features can provide spatial information for our final predictions at the bottom layer. Therefore, the multi-scale feature is quite important to assist saliency detection. As shown in Fig. 2, these convolution blocks below in side outputs are processed by VGG-16 first five convolutional blocks. The function of these convolution blocks is to obtain different scale features $\{X_1, X_2, X_3, X_4, X_5\}$. Each of convolution block use kernel size of 3×3 and outputs features with 128 channels.

1) *Contrast Features*: Saliency detection is related to the global or local contrast of foreground and background. Whether saliency objects are easy to detect is very important. For salient objects in an image, salient objects are the foreground that highlights the background around them. Salient features must be evenly distributed in the foreground, and the foreground and background regions are different. In order to capture such contrast information, we add contrast features related to each stage edge feature X_i^F , the feature X_i^F is output by guidance block. Each contrast feature is computed by subtracting X_i^F from its local average, the kernel size is 3×3 . Through average pooling operation that can reduce the error caused by the variance of the estimated value due to the limitation of the size of the neighborhood, and retain more background information of the image. Hence subtract $\text{AvgPool}(X_i^F)$ can retain more foreground information, salient objects are easier to detect.

$$X_i^c = X_i^F - \text{AvgPool}(X_i^F) \quad (1)$$

2) *Deconvolution Features*: After the last step, the size of the five contrast features is gradually decreasing. The first size of contrast feature X_1^c is 176×176 , but the fifth size of contrast feature X_5^c is 11×11 , in order to obtain the same size of final output 176×176 need from back to front sequentially use five deconvolution layers to increase the size of precomputed feature maps X_i^F and X_i^c . At each Deconv blocks, we upsample the previous feature by the stride of 2. The result of the deconvolution feature map D_i is computered by combining the information of edge feature X_i^F and local contrast feature X_i^c , feature D_i by unsampled will obtain feature D_{i+1} . The Deconv operation is achieved by deconvolution layer with the kernel size is 5×5 the stride of 2. The input of this layer is the concatenation of X_i^F, X_i^c

and D_{i+1} and the channels number of D_{i+1} is sum of X_i^F and D_{i+1} .

$$D_i = \text{Deconv}(X_i^F, X_i^c, D_{i+1}) \quad (2)$$

3) *Local Features*: The Local block use a convolution layer with a stride of 1 and a kernel size of 1×1 to get the final local features maps X_L . Through concatenate operation to fusion feature of X_1^F , X_1^c and D_2 . Samely, the channels number of X_L is the sum of X_1^F and D_2 . The local feature X_L size is 176×176 , for convenience to fusion with the global feature, we need again use Deconv operation to increase local feature X_L size of 176×176 to 352×352 .

$$X_L = \text{Conv}(X_1^F, X_1^c, D_2) \quad (3)$$

4) *Global Features*: A good saliency detection model not only can capture local features but also can capture global features. Before assigning saliency tasks to a single small region, the saliency model needs to capture the global context of the image. To achieve this purpose, we use three convolution layers after the last VGG block to computer global feature X_G . The first two convolution layers use a kernel size of 5×5 , the last convolutional layer uses a kernel size of 3×3 and all convolutional layers have the same channels.

C. Edge Guidance Block

The inspiration of edge guidance block comes from [23], this paper employs deep spatial feature transform to recovery realistic texture in image super-resolution, they use the possibility of semantic segmentation maps as the categorical prior, an spatial feature transform layer is conditioned on semantic segmentation probability maps, based on it super-resolution results can be improved. Similar to it but different from it, as shown in Fig. 2, Our edge guidance block is composed of two stage. Because through five side outputs will obtain five different scale features with different channels, to effectively fusing features (X_i, X_i^E) and use few parameters inside each guidance block and increased collaboration among network layers. we use a Condition Network(CN) to generate shared intermediate condition that can be broadcasted to all edge guidance blocks. In the first stage, our Condition Network(CN) use four convolutional layers, each convolutional layer with a kernel size of 3×3 and a stride of 1. Through CN each an edge map through four convolution operation mapping edge features into high dimensional space and will obtain a intermediate condition X_i^E and the condition's size is 176×176 . The above-mentioned CN can produce coarse edge feature X_i^E . In order to better transfer edge features to the next layer of the network, play a better guidance role. We propose a guidance block to embed edge prior knowledge into hierarchical feature maps. The guidance block uses two separate branches that output two features (γ, β) base on CN. The feature X_i^E and feature γ through multiply operation obtained middle feature, the middle feature and feature β through add operation obtained feature X_i^F . Since the spatial dimensions are preserved, the guidance block not only performs feature-wise manipulation but also spatial-wise transformation. Existing methods about saliency detection only use the side output through channel-wise operation(concatenation or addition) but ignore the importance

of global context and local detail information. So we combine the non-local feature to fill the deficiency.

$$EGB(X_i^F | \gamma, \beta) = X_i^E \odot \gamma + \beta \quad (4)$$

where \odot represents multiply operation and $+$ represents add operation.

D. Loss Function

Saliency detection and image segmentation usually come down to the optimization of non-convex energy functions consisting of data items and regularization items. A mathematical global model is the Mumford-Shah(MS) model [44], it transforms the image segmentation problem into solving the minimum value of energy function. By constructing the energy function, the curve is evolved under the driving of the minimum value of energy function and the contour curve gradually approaches the boundary of the object, and finally, the object is segmented. In [20] proposed a supervised deep convolutional network, the loss function approximates the MS functional are made of a cross entropy loss term between ground truth and predicted the saliency map and boundary loss term. The purpose of MS functional is to minimize IOU loss by maximizing the coincidence rate between predicted boundaries and real boundaries.

$$F_{MS} \approx \underbrace{\sum_j \lambda_j \int_{v \in \Omega_j} S_j(y(v), \hat{y}(v)) dv}_{\text{cross entropy loss}} + \underbrace{\sum_j \gamma_j (1 - IoU(C_j, \hat{C}_j))}_{\text{boundary loss}} \quad (5)$$

where v is the pixel location, S_j is the total loss between ground truth (y) and predicted (\hat{y}) saliency map, and $IoU(C_j, \hat{C}_j)$ is the intersection over union between the true boundary and predicted boundary. The positive constant λ_j , and γ_j tune the multi-criteria energy function in terms of data fidelity and total boundary length.

1) *Cross-entropy Loss*: We use two linear operators (W_G, b_G) and (W_L, b_L) to combine the local and global features. And the softmax function is used to compute the probability for each pixel of being salient or not.

$$\hat{y} = p(y(v) = s) = \frac{e^{W_L^s X_{L(v)} + b_L^s} + e^{W_G^s X_{G(v)} + b_G^s}}{\sum_{s' \in \{0,1\}} e^{W_L^{s'} X_{L(v)} + b_L^{s'}} + e^{W_G^{s'} X_{G(v)} + b_G^{s'}}} \quad (6)$$

where p is the probability for each pixel of being salient, v is the location of a pixel and s indicates that the pixel belongs to the foreground. The cross-entropy loss function is:

$$G_j(y(v), \hat{y}(v)) = -\frac{1}{N} \sum_{i=1}^N \sum_{s \in \{0,1\}} (y(v_i) = s) (\log(\hat{y}(v_i = s))) \quad (7)$$

where $y(v)$ is the ground truth and $\hat{y}(v)$ is the predicted saliency map.

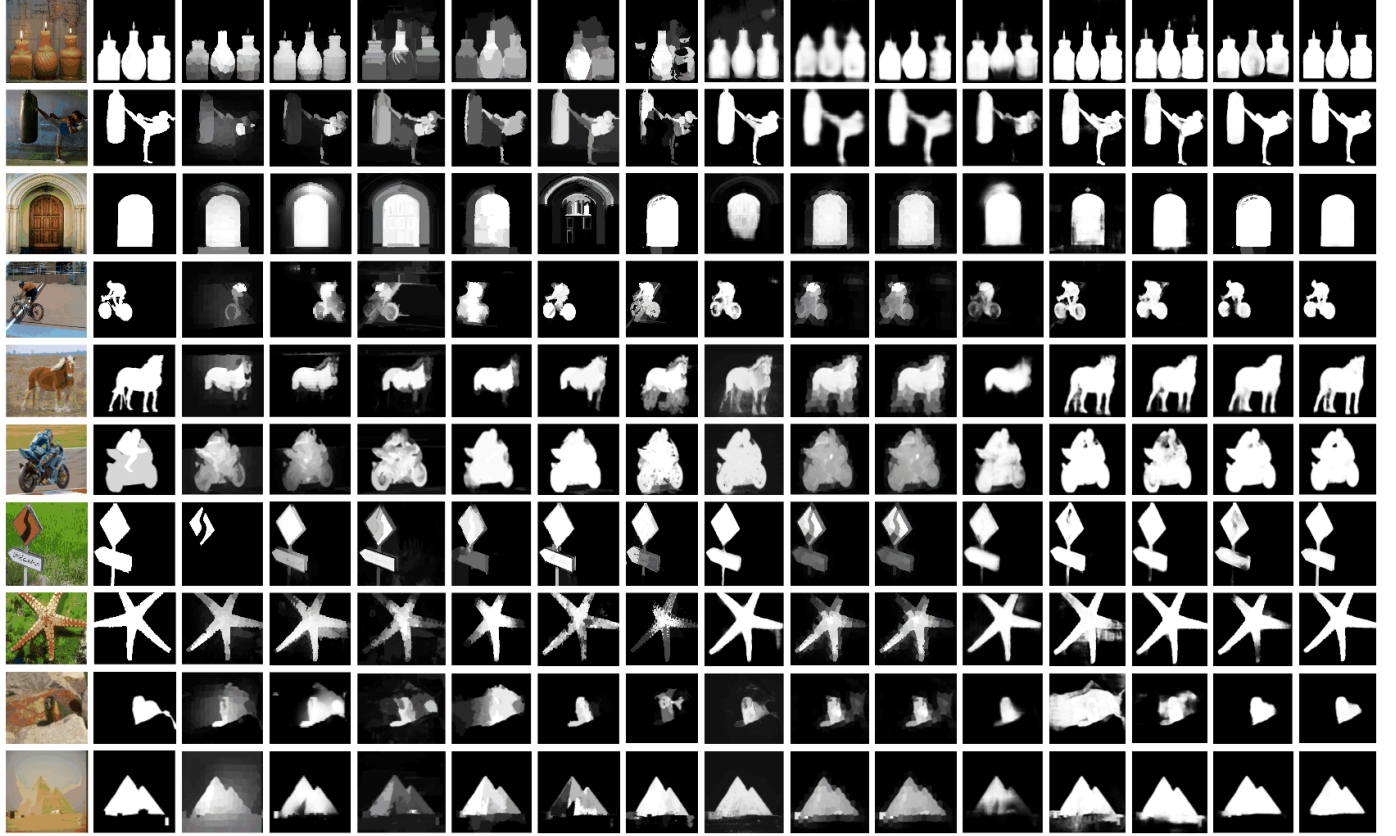


Fig. 3. Saliency maps produced by the MR[10], DRFI[45], wCtr[46], MCDL[30], MDF[25], DCL[15], DS[47], DSS[35], LEGS[31], UCF[48], WSS[49], Amulet[18] and NLDF[20], Our model can deliver state-of-the-art performance on five datasets.

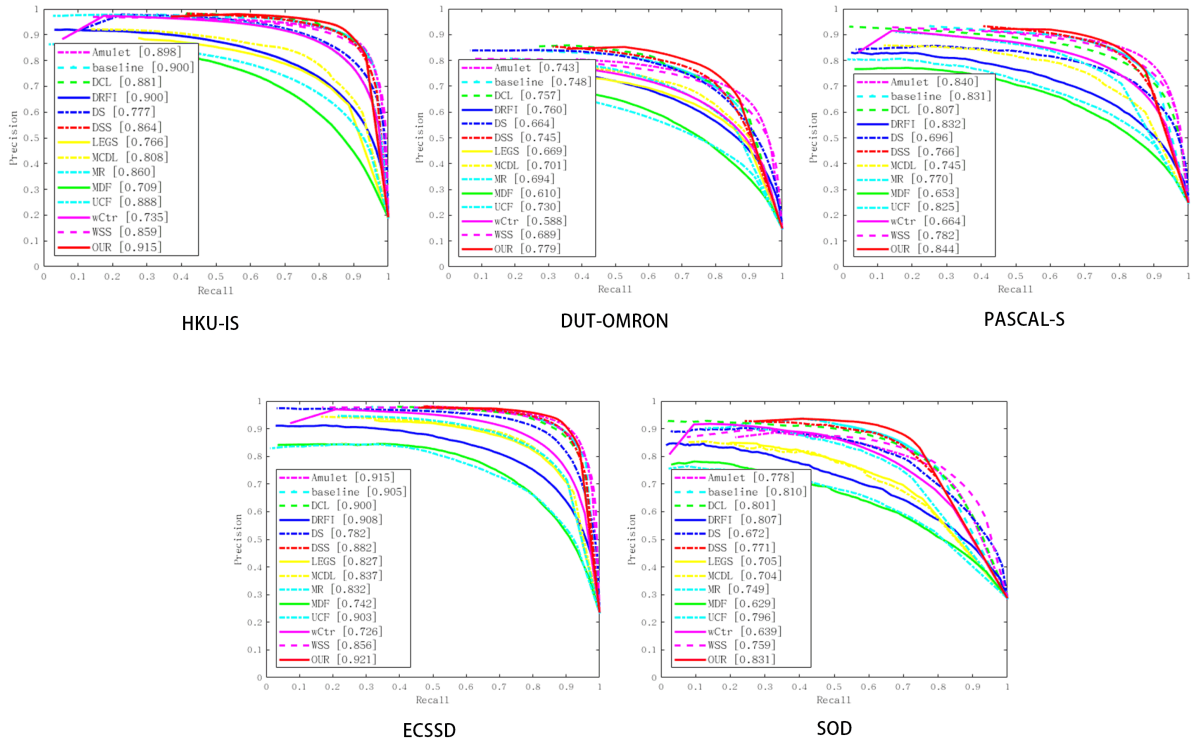


Fig. 4. Precision-recall curves for our model compared to MR[10], DRFI[45], wCtr[46], MCDL[30], MDF[25], DCL[15], DS[47], DSS[35], LEGS[31], UCF[48], WSS[49], Amulet[18], NLDF[20], Our model can deliver state-of-the-art performance on five datasets.

TABLE II

THE MAXIMUM F-MEASURE (LARGER IS BETTER) AND MAE (SMALLER IS BETTER) OF DIFFERENT SALIENCY DETECTION METHODS ON FIVE RELEASED SALIENCY DETECTION DATASETS.

*	HKU-IS		DUT-OMRON		PASCAL-S		ECSSD		SOD	
	max F_β	MAE								
OUR	0.915	0.040	0.779	0.065	0.843	0.095	0.921	0.051	0.831	0.134
NLDF	0.902	0.048	0.753	0.080	0.831	0.099	0.905	0.063	0.810	0.143
Amulet	0.899	0.050	0.743	0.098	0.839	0.099	0.915	0.059	0.778	0.156
WSS	0.858	0.079	0.689	0.110	0.782	0.141	0.856	0.103	0.759	0.181
UCF	0.888	0.061	0.730	0.120	0.825	0.115	0.903	0.069	0.796	0.159
LEGS	0.770	0.118	0.669	0.133	0.756	0.157	0.827	0.118	0.707	0.215
DSS	0.900	0.050	0.760	0.074	0.832	0.104	0.908	0.062	0.807	0.145
DS	0.864	0.078	0.745	0.120	0.766	0.176	0.882	0.122	0.771	0.199
DCL	0.892	0.054	0.733	0.084	0.815	0.113	0.887	0.072	0.795	0.142
MDF	0.861	0.076	0.694	0.092	0.764	0.145	0.832	0.105	0.745	0.192
MCDL	0.808	0.092	0.701	0.089	0.745	0.146	0.837	0.101	0.704	0.194
wCtr	0.735	0.138	0.588	0.171	0.664	0.199	0.726	0.165	0.639	0.231
DRFI	0.777	0.144	0.664	0.150	0.696	0.210	0.782	0.170	0.672	0.242
MR	0.709	0.174	0.610	0.187	0.653	0.232	0.742	0.186	0.629	0.274

2) *IoU Boundary Loss*: This inspiration comes from the applications of IOU boundary loss in image segmentation[50], [51]. IOU boundary loss computer the error between the true boundary C_j and predicted boundary \hat{C}_j , the boundary pixels using a Sobel operator followed by a tanh activation function and this active function predicts the gradient magnitude of saliency maps to a probability range of [0,1]. The IOU boundary loss can be represented as:

$$IoULoss = 1 - \frac{2 | C_j \cap \hat{C}_j |}{| C_j | + | \hat{C}_j |} \quad (8)$$

E. Implementation

We have implemented our network on a single Nvidia GTX 1070Ti GPU and in Tensorflow [52]. Pre-trained VGG-16 [33] is used to initialize the weights in first five VGG Blocks. All weights of convolution and deconvolution were initialized randomly with a constant(0.01), and the biases were initialized to 0. The learning rate is 10^{-5} and λ_j, γ_j in Eq.(5) were set to 1.

We training our model on MSRA-B [53] dataset and testing on five popular benchmarks. The same as the NLDF [20], we use horizontal flipping as data augmentation, resulting in an augmented image set with twice large than the original one. All training images are resized to 352×352 and use cross entropy loss and IOU boundary loss to optimizing our network. Without further optimization, the trained model is used to predict the saliency maps of other datasets. The whole training produces for 10 epochs with a single image batch size, it takes about ten hours to complete the whole training.

IV. EXPERIMENTS

A. Experimental Setup

Evaluation Datasets. We evaluate the proposed model on five public benchmark datasets: HKU-IS [25], PASCAL-S [26], DUT-OMRON [10], ECSSD [11] and SOD [27]. **HKU-IS**: This data set contains 4447 images with high quality pixel labeling, and most of the images have low contrast and many

salient objects. This data set contains many independent salient objects or objects touching the image boundary. **PASCAL-S**: This dataset has 850 natural images which are generated from the PASCAL VOC [54] segmentation challenge. The ground truth labeled by 12 experts contains both pixel-wise saliency and eye fixation. **DUT-OMRON**: This is a large data set with 5168 high quality images. Each image in this dataset has one or more salient objects and a cluttered background. Therefore, this data set is more difficult and challenging, which provides more space for improvement for the research of saliency detection. **ECSSD**: This dataset contains 1000 natural and complex images with pixel-wise ground truth annotations and these images are manually selected from the Internet. **SOD**: This dataset has 300 images, and it was originally designed for image segmentation. This dataset is challenging because many images have multiple objects which with low contrast or touching the image boundary.

Evaluation Criteria. We use three evaluation metrics to evaluation the performance of our model with other salient object detection methods. Precision-recall(PR) curves, F-measure score and mean absolute error(MAE)[55]. With continuous values normalized the saliency map to the range of 0 to 255, we compute the corresponding binary map, then computer the precision /recall pairs of all boundary maps in the dataset. The PR curve of a dataset explains the mean precision and recall of saliency maps at different thresholds. The F-measure is a harmonic mean of average precision and average recall, F-measure can be represented as:

$$F_\beta = \frac{(1 + \beta^2) \cdot Precision \cdot Recall}{\beta^2 \cdot Precision + Recall} \quad (9)$$

where $\beta^2=0.3$ to emphasize precision over recall the same as [56]. The mean absolute error (MAE) to measure the average difference between predicted saliency map S and ground truth G:

$$MAE = \frac{1}{W \times H} \sum_{x=1}^W \sum_{y=1}^H | S(x, y) - G(x, y) | \quad (10)$$

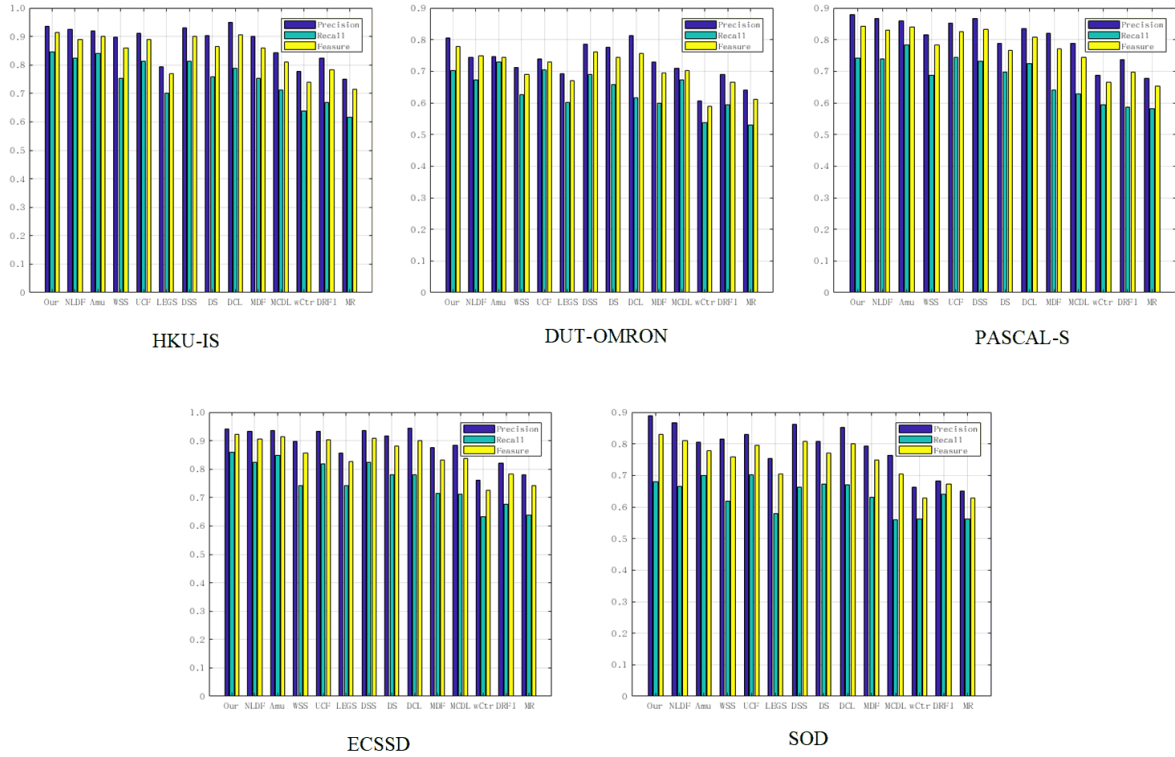


Fig. 5. For a better visual effect, we represent the Presion, Recall and F-measure value in the form of a histogram compared to MR [10], DRFI [45], wCtr [46], MCDL [30], MDF [25], DCL [15], DS [47], DSS [35], LEGS [31], UCF [48], WSS [49], Amulet [18], NLDF [20], Our model is in the first column can deliver state-of-the-art performance on five datasets.

where W and H is the width and height of a given image.

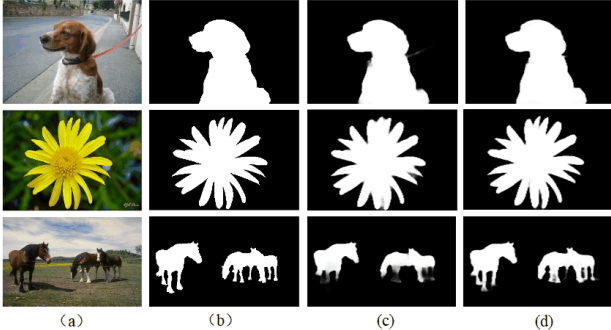


Fig. 6. An input image(a) with ground truth(b), without edge(c) and with edge(d)

B. Comparison with State-of-the-arts

We compare our method with other state-of-art ones including 3 conventional methods(MR [10], DRFI [45], wCtr [46]) and 10 deep learning based methods(MCDL [30], MDF [25], DCL [15], DS [47], DSS [35], LEGS [31], UCF [48], WSS [49], Amulet [18], NLDF [20]). For fair comparison, we use either the implementations with suggested parameter settings and the saliency maps provided by the authors.

TABLE III
THE EFFECT OF DIFFERENTS NUMBER OF GUIDANCE BLOCKS ON PERFORMANCE.

*	Five EFN		Three EFN		Zero EFN	
	$\max F_\beta$	MAE	$\max F_\beta$	MAE	$\max F_\beta$	MAE
HKU-IS	0.915	0.040	0.906	0.046	0.902	0.048
DUT-OMRON	0.779	0.065	0.772	0.077	0.753	0.080
PASCAL-S	0.843	0.095	0.839	0.098	0.831	0.099
ECSSD	0.921	0.051	0.913	0.057	0.905	0.063
SOD	0.831	0.134	0.828	0.136	0.810	0.143

C. Quatitive Evaluation

First, we compare the proposed methods with the others in terms of F-measure scores, MAE scores, and PR-curves. In Fig. 3 provides a visual comparison of our approach and other methods. It can be seen our method generates more clear saliency maps in various challenging images. What's more, our method can outperform other compared across all the datasets of all evaluation metrics. Our method improves the F-measure of on five datasets, especially on the large-scale dataset, such as DUT-OMRON and HKU-IS. PR-curves are shown in Fig.4 and the F-measure and MAE scores are shown in TABLE II. In order to express the superiority of our method more intuitively, we express the values of Precision, Recall and F-measure in the form of the histogram with five datasets and 13 methods, as shown in Fig.5.

D. Impact of Edge Guidance Block

In order to verify the effect of we proposed guidance block, the inclusion of edge feature in our model as compared to baseline for an increase in $\max F_\beta$ and decrease in MAE on HKU-IS, DUT-OMRON, PASCAL-S, ECSSD and SOD five datasets as shown in TABLE.II. It can be observed visualization results that without edge guidance block in the NLDF [20] are shown in Fig.3. With the help of guidance block, our approach can detect and better localize the edge of most salient objects. Several visual examples are illustrated in Fig.6. Meantime, to verify the effectiveness of embedding several numbers of edge guidance block. We have done three experiments, one is embedded in the five and three guidance blocks, the other is not embed edge guidance block. The experimental results show that the results of five embeddings are better, the results are shown in TABLE III.

E. Execution Time

Some methods to achieve more accurate results at the cost a longer running time. However, we achieve better performance while maintaining efficient runtime. When testing the model, our method maintains a reasonable reasonable runtime of 0.08s per image.

V. CONCLUSION

In this paper, we proposed a novel novel Edge-guided Non-local FCN (ENFNet) for salient object detection from the local and global perspective. We demonstrated that with saliency edge prior knowledge to perform edge-guided feature learning is beneficial to training and saliency inference. Through edge-related guidance block the edge features are embedded into our network, our network learned more accurate edge structure information, the edge features are able to effectively preserve sharp edges of salient objects and get the clear boundaries. The saliency detection results are improved compared to without edge guidance. Experimental results demonstrate that we proposed method consistently improves the performance on all five benchmarks and outperforms 13 state-of-art methods under different evaluation metrics.

REFERENCES

- [1] M. Donoser, M. Urschler, M. Hirzer, and H. Bischof, “Saliency driven total variation segmentation,” in *Proceedings of IEEE European Conference on Computer Vision*, 2009.
- [2] C. Li, L. Lin, W. Zuo, W. Wang, and J. Tang, “An approach to streaming video segmentation with sub-optimal low-rank decomposition,” *IEEE Transactions on Image Processing*, vol. 25, no. 5, pp. 1947–1960, 2016.
- [3] C. Li, X. Wang, L. Zhang, J. Tang, H. Wu, and L. Lin, “Weighted low-rank decomposition for robust grayscale-thermal foreground detection,” *IEEE Transactions on Circuits and Systems for Video Technology*, vol. 27, no. 4, pp. 725–738, 2017.
- [4] Z. Ren, S. Gao, L. Chia, and I. W. Tsang, “Region-based saliency detection and its application in object recognition,” *IEEE Transactions on Circuits System Video Technonogy*, vol. 24, no. 5, pp. 769–779, 2014.
- [5] A. Borji, S. Frintrop, D. N. Sihite, and L. Itti, “Adaptive object tracking by learning background context,” in *Proceedings of IEEE Conference on Computer Vision and Pattern Recognition Workshops*, 2012.
- [6] C. Li, H. Cheng, S. Hu, X. Liu, J. Tang, and L. Lin, “Learning collaborative sparse representation for grayscale-thermal tracking,” *IEEE Transactions on Image Processing*, vol. 25, no. 12, pp. 5743–5756, 2016.
- [7] C. Li, L. Lin, W. Zuo, J. Tang, and M. H. Yang, “Visual tracking via dynamic graph learning,” *IEEE Transactions on Pattern Analysis and Machine Intelligence*, 2019.
- [8] R. Zhao, W. Ouyang, and X. Wang, “Unsupervised salience learning for person re-identification,” in *Proceedings of IEEE Conference on Computer Vision and Pattern Recognition*, 2013.
- [9] F. Perazzi, P. Krähenbühl, Y. Pritch, and A. Hornung, “Saliency filters: Contrast based filtering for salient region detection,” in *Proceedings of IEEE Conference on Computer Vision and Pattern Recognition*, 2012.
- [10] C. Yang, L. Zhang, H. Lu, X. Ruan, and M. Yang, “Saliency detection via graph-based manifold ranking,” in *Proceedings of IEEE Conference on Computer Vision and Pattern Recognition*, 2013.
- [11] Q. Yan, L. Xu, J. Shi, and J. Jia, “Hierarchical saliency detection,” in *Proceedings of IEEE Conference on Computer Vision and Pattern Recognition*, 2013.
- [12] G. Lee, Y.-W. Tai, and J. Kim, “Deep saliency with encoded low level distance map and high level features,” in *Proceedings of IEEE Conference on Computer Vision and Pattern Recognition*, 2016.
- [13] G. Lee, Y. Tai, and J. Kim, “Deep saliency with encoded low level distance map and high level features,” in *Proceedings of IEEE Conference on Computer Vision and Pattern Recognition*, 2016.
- [14] L. Wang, H. Lu, X. Ruan, and M. Yang, “Deep networks for saliency detection via local estimation and global search,” in *Proceedings of IEEE Conference on Computer Vision and Pattern Recognition*, 2015.
- [15] G. Li and Y. Yu, “Deep contrast learning for salient object detection,” in *Proceedings of IEEE Conference on Computer Vision and Pattern Recognition*, 2016.
- [16] X. Shen and Y. Wu, “A unified approach to salient object detection via low rank matrix recovery,” in *Proceedings of IEEE Conference on Computer Vision and Pattern Recognition*, 2012.
- [17] Q. Hou, M. Cheng, X. Hu, A. Borji, Z. Tu, and P. H. S. Torr, “Deeply supervised salient object detection with short connections,” in *Proceedings of IEEE Conference on Computer Vision and Pattern Recognition*, 2017.
- [18] P. Zhang, D. Wang, H. Lu, H. Wang, and X. Ruan, “Amulet: Aggregating multi-level convolutional features for salient object detection,” in *Proceedings of IEEE International Conference on Computer Vision*, 2017.
- [19] X. Chen, A. Zheng, J. Li, and F. Lu, “Look, perceive and segment: Finding the salient objects in images via two-stream fixation-semantic cnns,” in *Proceedings of IEEE International Conference on Computer Vision*, 2017.
- [20] Z. Luo, A. K. Mishra, A. Achkar, J. A. Eichel, S. Li, and P. Jodoin, “Non-local deep features for salient object detection,” in *Proceedings of IEEE Conference on Computer Vision and Pattern Recognition*, 2017.
- [21] P. Mukherjee, B. Lall, and S. Tandon, “Salprop: Salient object proposals via aggregated edge cues,” in *Proceedings of IEEE International Conference on Image Processing*, 2017.
- [22] Y. Tang and X. Wu, “Saliency detection via combining region-level and pixel-level predictions with cnns,” in *Proceedings of IEEE Conference on European Conference on Computer Vision*, 2016.
- [23] X. Wang, K. Yu, C. Dong, and C. C. Loy, “Recovering realistic texture in image super-resolution by deep spatial feature transform,” in *Proceedings of IEEE Conference on Computer Vision and Pattern Recognition*, 2018.
- [24] C. L. Zitnick and P. Dollár, “Edge boxes: Locating object proposals from edges,” in *Proceedings of IEEE European Conference on Computer Vision*, 2014.
- [25] G. Li and Y. Yu, “Visual saliency based on multiscale deep features,” in *Proceedings of IEEE Conference on Computer Vision and Pattern Recognition*.
- [26] Y. Li, X. Hou, C. Koch, J. M. Rehg, and A. L. Yuille, “The secrets of salient object segmentation,” in *Proceedings of IEEE Conference on Computer Vision and Pattern Recognition*, 2014.
- [27] D. R. Martin, C. C. Fowlkes, D. Tál, and J. Malik, “A database of human segmented natural images and its application to evaluating segmentation algorithms and measuring ecological statistics,” in *Proceedings of IEEE European Conference on Computer Vision*, 2001.
- [28] L. Wang, L. Wang, H. Lu, P. Zhang, and X. Ruan, “Saliency detection with recurrent fully convolutional networks,” in *Proceedings of IEEE European Conference on Computer Vision*, 2016.
- [29] J. Kuen, Z. Wang, and G. Wang, “Recurrent attentional networks for saliency detection,” in *Proceedings of IEEE Conference on Computer Vision and Pattern Recognition*, 2016.
- [30] R. Zhao, W. Ouyang, H. Li, and X. Wang, “Saliency detection by multi-context deep learning,” in *Proceedings of IEEE Conference on Computer Vision and Pattern Recognition*, 2015.

- [31] L. Wang, H. Lu, X. Ruan, and M. Yang, "Deep networks for saliency detection via local estimation and global search," in *Proceedings of IEEE Conference on Computer Vision and Pattern Recognition*, 2015.
- [32] T. Wang, L. Zhang, S. Wang, H. Lu, G. Yang, X. Ruan, and A. Borji, "Detect globally, refine locally: A novel approach to saliency detection," in *Proceedings of IEEE Conference on Computer Vision and Pattern Recognition*, 2018.
- [33] K. Simonyan and A. Zisserman, "Very deep convolutional networks for large-scale image recognition," in *3rd International Conference on Learning Representations*, 2015.
- [34] S. Xie and Z. Tu, "Holistically-nested edge detection," in *Proceedings of the IEEE International Conference on Computer Vision*, 2015.
- [35] Q. Hou, M.-M. Cheng, X. Hu, A. Borji, Z. Tu, and P. H. Torr, "Deeply supervised salient object detection with short connections," in *Proceedings of the IEEE Conference on Computer Vision and Pattern Recognition*, 2017.
- [36] T. Wang, A. Borji, L. Zhang, P. Zhang, and H. Lu, "A stagewise refinement model for detecting salient objects in images," in *Proceedings of IEEE International Conference on Computer Vision*, 2017.
- [37] X. Wang, H. Ma, and X. Chen, "Salient object detection via fast R-CNN and low-level cues," in *Proceedings of IEEE International Conference on Image Processing*, 2016.
- [38] X. Wang, H. Ma, X. Chen, and S. You, "Edge preserving and multi-scale contextual neural network for salient object detection," *IEEE Transactions Image Processing*, vol. 27, no. 1, pp. 121–134, 2018.
- [39] A. D. Sappa and F. Dornaika, "An edge-based approach to motion detection," in *Computational Science International Conference, Reading*, 2006.
- [40] J. Zhang, Y. Dai, F. Porikli, and M. He, "Deep edge-aware saliency detection," *CoRR*, vol. abs/1708.04366, 2017.
- [41] J. Liu, Q. Hou, M. Cheng, J. Feng, and J. Jiang, "A simple pooling-based design for real-time salient object detection," *Computer Research Repository*, vol. abs/1904.09569, 2019.
- [42] W. Guan, T. Wang, J. Qi, L. Zhang, and H. Lu, "Edge-aware convolution neural network based salient object detection," *IEEE Signal Processing Letters*, vol. 26, no. 1, pp. 114–118, 2019.
- [43] P. O. Pinheiro, T. Lin, R. Collobert, and P. Dollár, "Learning to refine object segments," in *Proceedings of IEEE Conference on European Conference on Computer Vision*, 2016.
- [44] Mumford, David, Shah, and Jayant, "Optimal approximations by piecewise smooth functions and associated variational problems," *Communications on Pure and Applied Mathematics*, vol. 42, no. 5, p. 577, 1989.
- [45] H. Jiang, J. Wang, Z. Yuan, Y. Wu, N. Zheng, and S. Li, "Salient object detection: A discriminative regional feature integration approach," in *Proceedings of IEEE Conference on Computer Vision and Pattern Recognition, Portland*, 2013.
- [46] W. Zhu, S. Liang, Y. Wei, and J. Sun, "Saliency optimization from robust background detection," in *Proceedings of IEEE Conference on Computer Vision and Pattern Recognition*, 2014.
- [47] X. Li, L. Zhao, L. Wei, M. Yang, F. Wu, Y. Zhuang, H. Ling, and J. Wang, "Deepsaliency: Multi-task deep neural network model for salient object detection," *IEEE Transactions Image Processing*, vol. 25, no. 8, pp. 3919–3930, 2016.
- [48] P. Zhang, D. Wang, H. Lu, H. Wang, and B. Yin, "Learning uncertain convolutional features for accurate saliency detection," in *Proceedings of IEEE International Conference on Computer Vision*, 2017.
- [49] L. Wang, H. Lu, Y. Wang, M. Feng, D. Wang, B. Yin, and X. Ruan, "Learning to detect salient objects with image-level supervision," in *Proceedings of IEEE Conference on Computer Vision and Pattern Recognition*, 2017.
- [50] F. Milletari, N. Navab, and S. Ahmadi, "V-net: Fully convolutional neural networks for volumetric medical image segmentation," in *Fourth International Conference on 3D Vision*, 2016.
- [51] A. A. Taha and A. Hanbury, "Metrics for evaluating 3d medical image segmentation: analysis, selection, and tool," *BMC Medical Imaging*, vol. 15, p. 29, 2015.
- [52] M. Abadi, A. Agarwal, P. Barham, E. Brevdo, Z. Chen, C. Citro, G. S. Corrado, A. Davis, J. Dean, M. Devin, S. Ghemawat, I. J. Goodfellow, A. Harp, G. Irving, M. Isard, Y. Jia, R. Józefowicz, L. Kaiser, M. Kudlur, J. Levenberg, D. Mané, R. Monga, S. Moore, D. G. Murray, C. Olah, M. Schuster, J. Shlens, B. Steiner, I. Sutskever, K. Talwar, P. A. Tucker, V. Vanhoucke, V. Vasudevan, F. B. Viégas, O. Vinyals, P. Warden, M. Wattenberg, M. Wicke, Y. Yu, and X. Zheng, "Tensorflow: Large-scale machine learning on heterogeneous distributed systems," *Computer Research Repository*, vol. abs/1603.04467, 2016.
- [53] T. Liu, Z. Yuan, J. Sun, J. Wang, N. Zheng, X. Tang, and H. Shum, "Learning to detect a salient object," *IEEE Trans. Pattern Analysis Machine Intelligence*, vol. 33, no. 2, pp. 353–367, 2010.
- [54] Everingham, Mark, Winn, and John, "The pascal visual object classes challenge 2007 (voc2007) development kit," *International Journal of Computer Vision*, vol. 111, no. 1, pp. 98–136, 2006.
- [55] A. Borji, D. N. Sihite, and L. Itti, "Salient object detection: A benchmark," in *Proceedings of IEEE Conference on European Conference on Computer Vision*, 2012.
- [56] R. Achanta, S. S. Hemami, F. J. Estrada, and S. Süsstrunk, "Frequency-tuned salient region detection," in *Proceedings of IEEE Conference on Computer Vision and Pattern Recognition*, 2009.